Design of model-based controllers for a class of nonlinear chaotic systems using a single output feedback and state observers

Ashraf A. Zaher
Physics Department, Science College, Kuwait University, P.O. Box 5969, Safat 13060, Kuwait
(Received 11 February 2007; revised manuscript received 29 March 2007; published 8 May 2007)

A model-based control methodology for suppressing chaos for nonlinear systems is introduced. The proposed methodology generates new periodic orbits or steady states, which are not the solutions of the free system, using output feedback and state observers. The design uses the certainty equivalence principle to construct a linear closed loop system that can follow desired outputs with zero steady state offsets via using a pole-placement-like approach. The combined dynamics of both the controller and the state observer are carefully studied using the well-known Rössler system. The similarities and differences between the proposed control technique and both the double-notch filter feedback and the time-delay autosynchronization are investigated. The effect of parameter uncertainties is studied and robustness of the proposed controller is analyzed.

DOI: 10.1103/PhysRevE.75.056203 PACS number(s): 05.45.Gg, 05.45.Pq

I. INTRODUCTION

Controlling the chaotic behavior of nonlinear systems has been an active area of research for the past two decades [1]. During the past 15 years, extensive studies on controlling chaos have been reported in the literature. The Ott-Grebogi-Yorke (OGY) method, developed in [2], introduced a controller that stabilizes unstable periodic orbits (UPOs) using small feedback perturbations to an accessible parameter. The control method relies on using an approximation for Poincaré map of the system, thus requiring the use of computer-based calculations, A/D and D/A converters, which is a limiting factor when applied to fast system. Another drawback is that noise can result in occasional bursts where the trajectory of the system is far from the controlled periodic orbit.

Adaptive control algorithms have been successfully applied to the control and synchronization of chaotic systems [3–5]. The design procedure achieves the desired objectives by constructing a suitable Lyapunov function and forcing its derivative to be negative (semi) definite. However, the construction of Lyapunov functions remains to be a difficult task, and is usually considered a bottleneck in the design of the control law.

Backstepping, a recursive design procedures, can extend the applicability of Lyapunov-based deigns to nonlinear systems via considering some of the state variables as virtual controls [6]. Backstepping designs are flexible and do not force the designed system to appear linear. They also avoid cancellation of, perhaps, useful nonlinearities and often introduce additional nonlinear terms to improve the transient performance [7]. Backstepping designs can have an over-parametrized structure; thus, some of the controller parameters can be used to improve the transient performance of the closed loop, while other parameters can be used to guarantee the asymptotic stability [8,9].

Double-notch filter feedback (DNFF), a nonmodel-based approach, is a simple, yet efficient, method for stabilizing steady states of chaotic systems. This technique proved to be very efficient for stabilizing fast dynamics because it can be easily implemented using simple analog hardware [10]. The parameters of the feedback controller are constants, but they can be chosen to change chaotic motion into a desired periodic motion or to suppress a selected frequency from the power spectrum of the system.

Time-delay autosychronization (TDAS) is another nonmodel-based approach that can achieve continuous control of chaotic nonlinear systems without the need of either complicated computer processing or sophisticated hardware [11]. The feasibility of the real-time applicability of TDAS has been experimentally verified in a wide variety of fields [12,13]. TDAS allows a noninvasive stabilization of UPOs as the control signal vanishes when the target attractor is reached. TDAS is especially superior when applied to systems that have very fast dynamics and low dimensions [14]. Other variants of this control strategy are reported in the literature to improve its performance and to overcome some of its limitations [15–17].

When developing model-based control systems, analysis of physical systems usually involves two steps: developing the mathematical models for the physical systems that accurately represent their behavior and predicting the behavior of these systems based on the derived models. When the true parameters of the systems are unknown, the controller parameters are either estimated directly (direct scheme) or computed by solving the same design equations with plant parameters estimates (indirect scheme). The resulting controller is called a certainty equivalence controller (CEC). The certainty equivalence principle is extended to controllers that use observers to have access to the unmeasured states. When only one or few states are available for direct measurements, the rest can be estimated using state observes that minimize a certain cost function using both linear and nonlinear techniques [18,19]. In this paper, a CEC controller is proposed that uses a simple gradient descent algorithm to observe the unmeasured states of the system. The dynamics of the state observer are the same as that of the original model with the addition of the auxiliary term that minimizes the error between the measured output and its estimate.

The rest of this paper is organized as follows. In Sec. II, the mathematical structure of the model describing nonlinear systems that are candidate to the proposed controller is in-

troduced. Section III deals with a systematic analytical derivation of the control law combined with the design of the states observers. In Sec. IV, the Rössler system is used to exemplify the application of the proposed controller. The dynamics of the Rössler system is investigated in Sec. IV A, and then two cases are considered illustrating stabilizing the system at a constant steady state (regulation), or an unstable periodic orbit (servomechanism) in Secs. IV B and IV C, respectively. In addition, the advantages and limitations of the proposed controller are highlighted via comparing its performance against two well-known controllers, DNFF and TDAS for the regulation and servomechanism cases respectively. Section V discusses some of the robustness measures when applying the proposed controller, and investigates the effect of parameters uncertainties on the closed loop performance. A conclusion is given in Sec. VI summarizing the analysis and design of the proposed controller.

II. PROBLEM FORMULATION AND MODELING OF NONLINEAR SYSTEMS

Consider a nonlinear model of the form

$$\dot{X} = f(X,t,u), \quad X = [x_i], \quad i = 1,2,\ldots,n, \quad \text{and } y = x_j, \tag{1}$$

$$j \in i,$$

where X is the state vector, t is the time, u is the control signal, n is the system order, and y is the output and the only measurable state of the system. The dynamics of the nonlinear system is further constrained to follow the structure illustrated in Eq. (2):

$$\dot{x}_i = f_i(X,t) = f_{L(i)}(X,t), \quad i = 1,2,\ldots,n-1,$$

$$\dot{x}_n = f_n(X,t) + u = f_{L(n)}(X,t) + f_{NL}(X,t) + u, \tag{2}$$

where $f_{L(i)} = \Sigma_{j=1}^{n} \alpha_{i,j} x_j, i = 1,2,\ldots,n$ is a linear function of the states, α is constant vector, and the nonlinear dynamics of the system are encapsulated in $f_{\mathrm{NL}}(X,t)$. Many real-world applications fall into the structure of the nonlinear system given by Eqs. (1) and (2). Among them two-well potential systems and Duffing oscillators [6,7,20], Rössler- and Lorenz-like systems [11,16], Colpitts, Chua, and Toda oscillators [3,21,22], and others [23]. When analyzing the behavior of such systems near equilibrium points, linearization techniques can be used to estimate the corresponding Lyapunov exponents as a quantitative measure of the system response.

In the absence of the control signal u the system undergoes a sequence of period doubling starting from a single limit cycle until it becomes chaotic, if one (some) of its parameters is (are) allowed to change monotonically. For some sets of the system parameters, the output will always experience chaos that is characterized by a number of UPOs embedded within the chaotic motion, regardless of the initial conditions. The model of the system is seen to be divided into two parts, linear and nonlinear. The goal of this paper is to stabilize the system response so that the output can settle down to either a fixed steady state or a single periodic orbit. This will be achieved by designing a model-based controller that can estimate the nonlinear part of the model and hence arrive at a new, completely linear, abstract level to model the system. Using certainty equivalence principle, a pole-placement controller is then designed to achieve the required asymptotic response with a prescribed model-reference-like behavior.

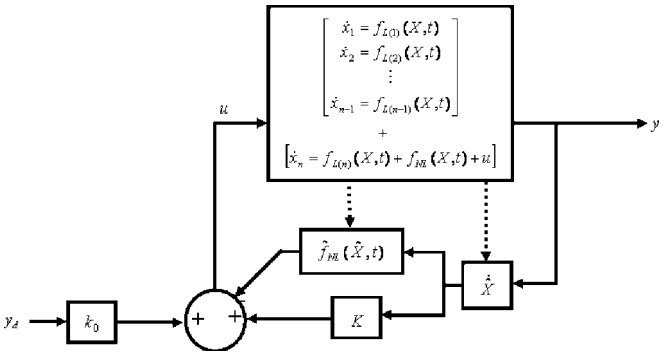

FIG. 1. Closed loop block diagram of the proposed controller. The dashed arrow indicates that the model structure and the control signal are passed to the dynamics describing the observed states.

III. DESIGN OF THE CONTROL LAW

The proposed control law has two goals. The first one is to cancel the nonlinearity via observing the immeasurable states of the system, while the second goal is to implement a linear full-state feedback to force the output of the system y to follow a desired trajectory y_d. The augmented dynamic system describing the control signal and the state observer is given by

$$u = -\hat{f}_{NL}(\hat{X},t) + K\hat{X} + k_0 y_d,$$

$$\dot{\hat{x}}_i = \hat{f}_i(\hat{X},t) + \gamma_i(y - \hat{y}), \quad i = 1,2,\ldots,n-1,$$

$$\dot{\hat{x}}_n = \hat{f}_n(\hat{X},t) + u + \gamma_n(y - \hat{y}), \tag{3}$$

where $\hat{X}$ is the estimated state vector, K is a vector of designed fixed parameters, k_0 is used to eliminate the steady state offset between both the actual output and its desired value, and $\Gamma = [\gamma_i]$ is a constant vector that is used to adjust the convergence rate of the observed states. As depicted in Eq. (3), a simple gradient descent algorithm is used to implement the state observer where $\hat{y}$ is the estimated output, $\hat{f}_{\mathrm{NL}}$ is the estimate of the nonlinear function, and $\hat{f}_i$ is the estimate of the system model given by Eqs. (1) and (2). Figure 1 shows a block diagram realization of the closed loop systems described by Eqs. (1)–(3).

Using certainty equivalence principle and assuming that the observed states of the system will asymptotically converge to their true values, we have

$$(\hat{X} \to X) \Rightarrow \{\hat{f}_{NL}(\hat{X},t) \to f_{NL}(X,t)\} \Rightarrow \dot{X} = AX + By_d, \quad (4)$$

where

$$A = [a_{i,j}] = \begin{bmatrix} \alpha_{1,1} & \alpha_{1,2} & \cdots & \alpha_{1,n-1} & \alpha_{1,n} \\ \alpha_{2,1} & \alpha_{2,2} & \cdots & \alpha_{2,n-1} & \alpha_{2,n} \\ \vdots & \vdots & \ddots & & \vdots \\ \alpha_{n-1,1} & \alpha_{n-1,2} & & \ddots & \alpha_{n-1,n} \\ \alpha_{n,1} + k_1 & \alpha_{n,2} + k_2 & \cdots & \alpha_{n,n-1} + k_{n-1} & \alpha_{n,n} + k_n \end{bmatrix}, \quad (5)$$

and

$$B = [b_i] = \begin{bmatrix} 0 \\ 0 \\ \vdots \\ \vdots \\ k_0 \end{bmatrix}.$$

IV. CASE STUDY

During the study of nonlinear dynamics, such as chaos and bifurcation, several benchmark models are used to exemplify the technique used to control the system. These benchmark models are always characterized by low dimensions to simplify the analysis, validation and verification of the proposed technique. The Rössler, Lorenz, Duffing oscillator, Van der Pol oscillator, and Chua's circuit are typical examples of such models. Interestingly, these models can always be cast in the form given by Eqs. (1) and (2). In this paper, the Rössler system is used as a case study to demonstrate the analysis and control of chaos, for which the dynamic model is described by

$$\dot{x}_1 = f_1(x_1,x_2,x_3,u) = -x_2 - x_3,$$

$$\dot{x}_2 = f_2(x_1,x_2,x_3,u) = x_1 + ax_2,$$

$$\dot{x}_3 = f_3(x_1,x_2,x_3,u) = -cx_3 + (b + x_1x_3) + u, \quad (6)$$

where $X=[x_1,x_2,x_3]^T$ is the state vector, u is the input, $y=x_2$ is the output, $a=0.2$ and $c=5.7$ are deterministic parameters, and b is an uncertain parameter that is governed by the following relationship:

$$b_{\min} \leqslant b \leqslant b_{\max}, \quad (7)$$

where $b_{\min}=0.15$ and $b_{\max}=0.25$. Comparing Eq. (6) with Eqs. (1) and (2), the following relationships are established: $f_{L1}=-x_2-x_3$, $f_{L2}=x_1+ax_2$, $f_{L3}=-cx_3$, and $f_{NL}=b+x_1x_3$. The nominal equilibrium points corresponding to $\dot{x}_1=\dot{x}_2=\dot{x}_3=u=0$ and $b=0.2$ are $X_{\text{eq}}=[5.6930,-28.4649,28.4649]^T$ and $[0.00702,-0.0351,+0.0351)]^T$ and the corresponding Lyapunov exponents are $\lambda_1 \cong \pm 5.4280i, 0.1930$ and $\lambda_2 \cong 0.0970 \pm 0.9952i, -5.6870$, respectively. The system will exhibit chaos with a dominant UPO of 5.86 s approximately.

A. Design of the control law

With reference to Eq. (3), the proposed control structure is

$$u = -(b + \hat{x}_1\hat{x}_3) + K[\hat{x}_1\ \hat{x}_2\ \hat{x}_3]^T + k_0y_d, \quad K = [k_1\ k_2\ k_3],$$

$$\dot{\hat{x}}_1 = -\hat{x}_2 - \hat{x}_3 - \gamma_1(\hat{x}_2 - x_2),$$

$$\dot{\hat{x}}_2 = \hat{x}_1 + a\hat{x}_2 - \gamma_2(\hat{x}_2 - x_2),$$

$$\dot{\hat{x}}_3 = -c\hat{x}_3 + (b + \hat{x}_1\hat{x}_3) + u - \gamma_3(\hat{x}_2 - x_2), \quad (8)$$

where y_d is the desired output and $\hat{x}_1$, $\hat{x}_2$, and $\hat{x}_3$ are the observed states corresponding to x_1, x_2, and x_3, respectively. It is assumed that only x_2, the system output, is available for measurement. The closed loop system is now given by

$$\begin{bmatrix} \dot{X} \\ \dot{\hat{X}} \end{bmatrix} = \begin{bmatrix} A_X & A_{\hat{X}} \\ \Omega_X & \Omega_{\hat{X}} \end{bmatrix} \begin{bmatrix} X \\ \hat{X} \end{bmatrix} + \begin{bmatrix} \Delta_X \\ \Delta_{\hat{X}} \end{bmatrix}, \quad (9)$$

where

$$A_X = \begin{bmatrix} 0 & -1 & -1 \\ 1 & a & 0 \\ 0 & 0 & -c \end{bmatrix}, \quad A_{\hat{X}} = \begin{bmatrix} 0 & 0 & 0 \\ 0 & 0 & 0 \\ k_1 & k_2 & k_3 \end{bmatrix},$$

$$\Omega_X = \begin{bmatrix} 0 & \gamma_1 & 0 \\ 0 & \gamma_2 & 0 \\ 0 & \gamma_3 & 0 \end{bmatrix}, \quad \Omega_{\hat{X}} = \begin{bmatrix} 0 & -1-\gamma_1 & -1 \\ 1 & a-\gamma_2 & 0 \\ k_1 & k_2-\gamma_3 & k_3-c \end{bmatrix},$$

$$\Delta_X = [0\ 0\ k_dy_d + (x_1x_3 - \hat{x}_1\hat{x}_3)]^T, \quad \Delta_{\hat{X}} = [0\ 0\ k_dy_d]^T. \quad (10)$$

Using the certainty equivalence principle and assuming that the observed states will asymptotically converge to the correct system states, we have

$$\dot{X} = AX + By_d, \text{ where } A = (A_X + A_{\hat{X}}) \text{ and } B = [0\ 0\ k_0]^T. \quad (11)$$

Equation (11) illustrates that, after all transients die out, the performance of the closed loop system will asymptotically mimic that of a desired output with a convergence rate that is governed by the choice of the controller parameters k_i and γ_i, $i=1$, 2 and 3. Regarding steady state accuracy, k_0 should be adjusted properly to eliminate any offsets. Two cases are considered to illustrate both regulation and servomechanism, where the desired output is constant and a slowly time-varying function, respectively.

B. Case I: Regulation, $y_d=y_{SS}$

Stabilizing the closed loop system to a constant steady state y_{SS} is now illustrated. The choice of the controller parameters is greatly simplified if the characteristic polynomial $T_1(s)$ of the closed loop system is chosen to have the form

$$T_1(s) = s^3 + p_1s^2 + p_2s + p_3 = (s+p)(s^2 + 2\zeta\omega_ns + \omega_n^2), \quad (12)$$

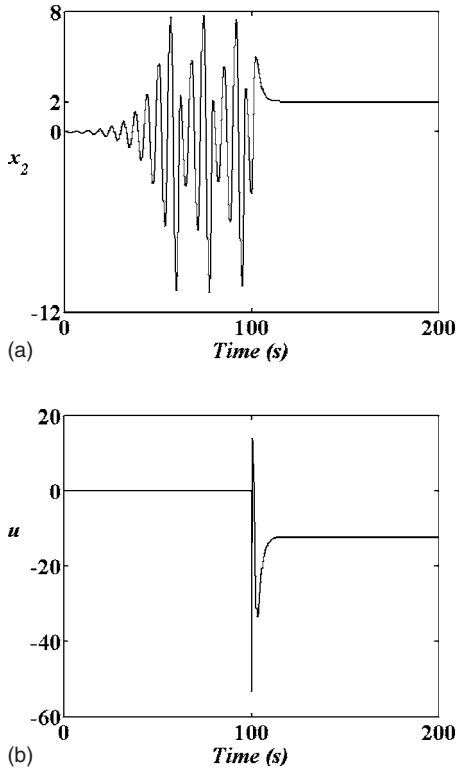

FIG. 2. The system's output, in (a), and control signal, in (b), of the closed loop system. The system is shown to reach a steady state in less than five seconds. The proposed controller was switched on at $t=100$ s.

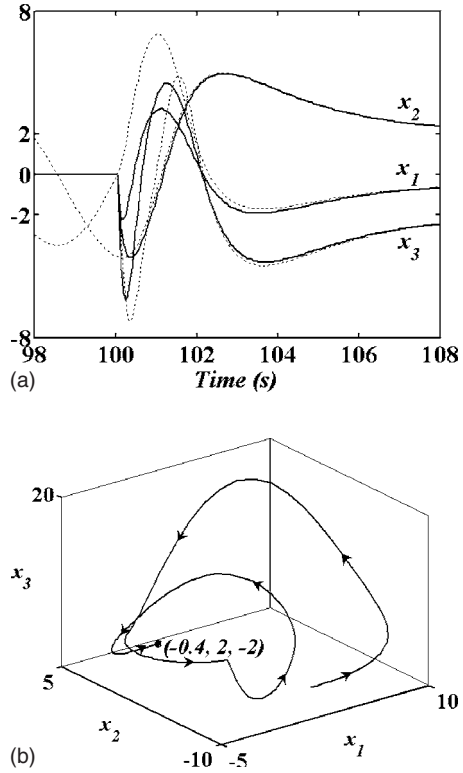

FIG. 3. Complete response of the closed loop system, in (a), showing the observed states (solid lines) converging very rapidly to the true states (dotted lines) of the system. The 3D phase plane, in (b), indicates that the desired operating point was reached with no offset.

$$p \gg \zeta\omega_n,$$

where p, p_1, p_2, and p_3 are positive constants characterizing the desired linear third order model, and ζ and ω_n are the damping ratio and natural frequency of the dominant behavior.

Thus matching Eq. (12) against the characteristic polynomial of A leads to

$$k_0 = -p_3, \quad k_1 = p_2 + ap_1 + a^2 - 1, \tag{13}$$

$$k_2 = p_3 + ap_2 + (a^2 - 1)p_1 + a(a^2 - 2), \quad k_3 = -p_1 + (c - a).$$

Figure 2 shows the response of the closed loop system for $y_d=2$, $p=10$, $\zeta=1$, and $\omega_n=1$. The parameters of the states observer were chosen to be $\gamma_1=\gamma_2=\gamma_3=10$, which are relatively large positive numbers to guarantee fast convergence of the observed states to their true values. Figure 3 illustrates the complete response of the closed loop system.

A conflict will always exist between the desired convergence rate and the control effort. If the controller is subject to saturation, the maximum value of $\Gamma=[\gamma_1\gamma_2\gamma_3]$ should be constrained in order not to introduce saturation nonlinearity into the closed loop system that might lead to undesirable sluggish performance.

Stabilization of steady states can also be achieved using two parallel notch filters. The DNFF damps all UPOs of the uncontrolled system by suppressing their corresponding power spectrum. A linear second order notch filter is given by

$$T_F(s) = \frac{Y_f(s)}{Y(s)} = \frac{k_f(s^2 + \omega_f^2)}{s^2 + \frac{\omega_f}{Q_f}s + \omega_f^2}, \tag{14}$$

where y_f, k_f, Q_f, ω_f are output, gain, quality factor, and resonance frequency in rad/s of the filter, respectively. Comparing the order and number of tunable parameters of both controllers reveals that the proposed model-based controller has an order of three and needs six parameters (K and Γ), while the DNFF has an order of four and needs six parameters (two sets of k_f, Q_f, and ω_f).

The DNFF performance depends crucially on the resonance frequencies and if chosen very close to the dominant frequency of the uncontrolled system, stabilization will fail [10]. In addition, for DNFF, steady state stabilization is only possible if the real part of the Lyapunov exponent is negative. These two shortcomings of the DNFF greatly affect its robustness and limit the scope of its applications. The proposed model-based controller does not suffer from these two problems, in addition, only the K vector needs to be analytically designed, as Γ is chosen empirically, implying that the design effort is reduced and robustness is increased. The DNFF is easily implemented in analog hardware and is, thus, suitable for applications having fast dynamics. In contrast,

the proposed model-based controller needs a digital-based implementation to reconstruct the estimated dynamics, which is a time-consuming process and is indeed a limiting factor when applied to real-world applications. Finally, although DNFF is a model-free design, extensive experimentation is required to choose Q_f and k_f in contrast to the systematic approach of choosing K of the proposed model-based controller.

C. Case II: Servomechanism, $y_d = A_0 \sin(\omega_0 t)$

In this case, the closed loop system will be stabilized to a periodic orbit that does not necessarily correspond to one of the UPOs embedded in the chaotic response of the uncontrolled system. The desired periodic orbit has amplitude of A_0 and a frequency of ω_0. Using the same technique illustrated in the previous section, the new characteristic polynomial, $T_2(s)$, of the closed loop system is now given by

$$T_2(s) = (s^2 + \omega_0^2) T_1(s). \tag{15}$$

Thus solving for k_0 is straightforward as conventional linear systems techniques can be utilized. Equation (16) illustrates the necessary steps to guarantee arriving at the necessary value of k_0 that will produce an output with the required amplitude A_0:

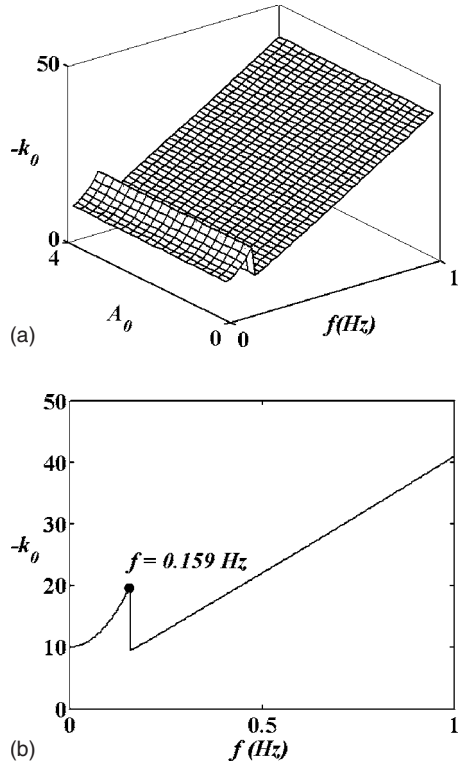

FIG. 4. Choosing k_0 for the servomechanism case. The 3D figure, in (a), shows k_0 as a function of the frequency and amplitude of the desired periodic orbit, while the other figure, in (b), is a cross sectional cut of the 3D figure illustrating the interaction between the desired periodic orbit frequency and the desired closed loop dynamics in $T_1(s)$. Notice the jump at $f=0.159$ Hz corresponding to $\omega_n = 1$ rad/s.

$$Y(s) = \frac{\varphi(s)}{T_1(s)} + \frac{\beta_1}{(s + j\omega_0)} + \frac{\beta_2}{(s - j\omega_0)} \Rightarrow Y_{SS}(s) = \frac{\beta_1}{(s + j\omega_0)} + \frac{\beta_2}{(s - j\omega_0)},$$

$$k_0 = \frac{-A_0 p_3}{\sqrt{\{\mathrm{Re}(\beta_1 + \beta_2) + \mathrm{Im}(\beta_1 + \beta_2)\}^2 + \{\mathrm{Re}(\beta_1 - \beta_2) + \mathrm{Im}(\beta_1 - \beta_2)\}^2}}, \tag{16}$$

where φ, β_1, and β_2 are the residues of $Y(s)$ and Re and Im stands for the real and imaginary parts of the complex residues, respectively. Figure 4 shows k_0 as a function of both A_0 and ω_0 of the desired periodic orbit where it is obvious that when ω_0 reduces to zero, the servomechanism case reduces to the regulation case where $A_0 = y_{SS}$.

Figure 5 illustrates the controlled response of the closed loop system for the case where $A_0=2$ and the desired period is 10 s corresponding to $\omega_0=0.628$ rad/s and $k_0=-13.975$. The rest of the controller parameters are the same as the regulation case. Extensive simulation results further prove that the system will follow any desired periodic orbit starting from any initial condition. The control signal is shown to settle down to a periodic function with the same frequency as that of the output. Figure 6 shows the complete response of the closed loop system.

Stabilizing UPOs can also be achieved using TDAS that is easily implemented without the exact model of either the controlled system or complicated computer processing for reconstruction of the underlying dynamics. For these two practical advantages, this control method has been successfully applied to experimental chaotic systems in various fields of research including electronic circuits, laser systems, mechanical oscillators, and chemical systems [12,13]. Both single and multiple TDAS provide a continuous linear control that is characterized by simple transfer functions. The controller of a single TDAS has the form

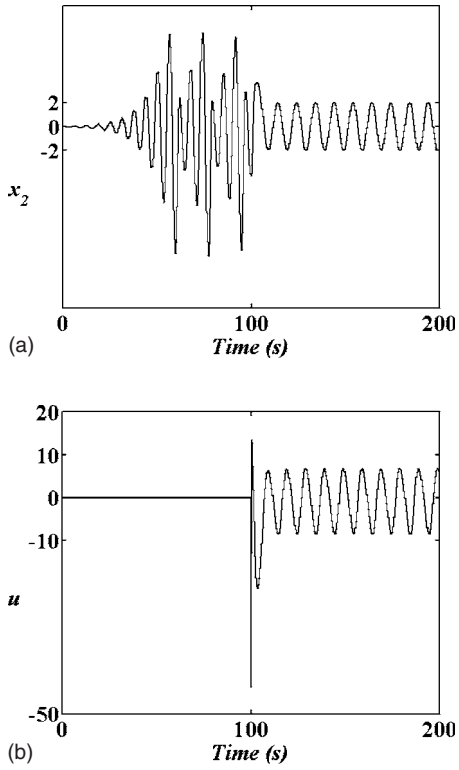

FIG. 5. Output, in (a), and control signal, in (b), of the closed loop system. The response of the system is seen to converge rapidly to the desired periodic orbit with the desired amplitude.

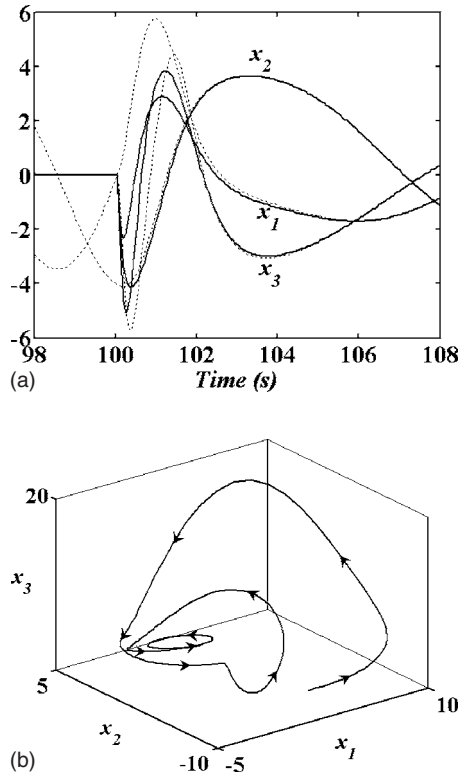

FIG. 6. Complete response of the closed loop system. The convergence rate, in (a), is very fast and almost identical to the results of the regulation case in Fig. 3. The 3D phase plane, in (b), further illustrates that the desired periodic orbit was reached with no offset.

$$u = k\{y(t-\tau) - y(t)\}, \tag{17}$$

where k is a constant gain and τ is the period of the UPO to be stabilized. The implementation of the controller is shown to be very simple and shares, with the DNFF, the advantage of being model-free and suitable for systems having fast dynamics. Using TDAS, the output converges to the desired periodic orbit while having noninvasive control as the control signal vanishes after stabilization. This is because the UPO survives the feedback, while the rest of the chaotic dynamics are damped out [15–17,24].

The convergence rate of the proposed controller is seen to be more flexible, but the control signal is invasive in contrast to that of the TDAS. Regarding the design effort, the TDAS needs only one parameter to be tuned k while the proposed controller needed six parameters K and Γ. One advantage of the proposed controller over the TDAS is the ability to stabilize the system to any periodic orbit, even if it does not exist among the original UPOs of the uncontrolled system. This is simply because the proposed controller cancels the unwanted nonlinearity of the uncontrolled system, which is the source of chaos, while the TDAS attempts to damp out all UPOs except the desired one. In addition, traditional TDAS controllers suffer from the so-called odd number condition that limits their use. The odd number condition gives a class of UPOs that cannot be stabilized by this control method. To overcome this problem and improve the controller performance, several variants of TDAS control method were introduced [17,25]. The proposed controller, in this paper, does not suffer from this problem and can be applied to virtually all nonlinear systems having the model structure depicted in Eqs. (1) and (2). The systematic approach in designing the controller parameters for the proposed model-based controllers is an added advantage over the TDAS, as it has been proven that it is very difficult to choose both k and τ [17,26]. Finally, controlling both the amplitude and frequency of the desired periodic orbit (steady state) is much easier and straightforward using the proposed controller than both DNFF and TDAS.

V. ROBUSTNESS ANALYSIS OF THE PROPOSED CONTROLLER

Addressing uncertainties and their effect on the closed-loop performance has been an active area of research that often led to the design of tracking controllers with the purpose of minimizing the effect of these uncertainties on the output. Varieties of techniques have been developed such as adaptive nonlinear control [27], nonlinear robust control using Lyapunov-based techniques [28], and model predictive control [29]. Intelligent control methods, based on artificial neural networks and fuzziness, are also found in the literature that rely on black-box modeling in a attempt to capture the nonlinear behavior of the system in terms of look-up tables and/or complex interconnections [30]. State feedback controllers are sometimes not suited for practical applications, as some of the states might not be available for direct measure-

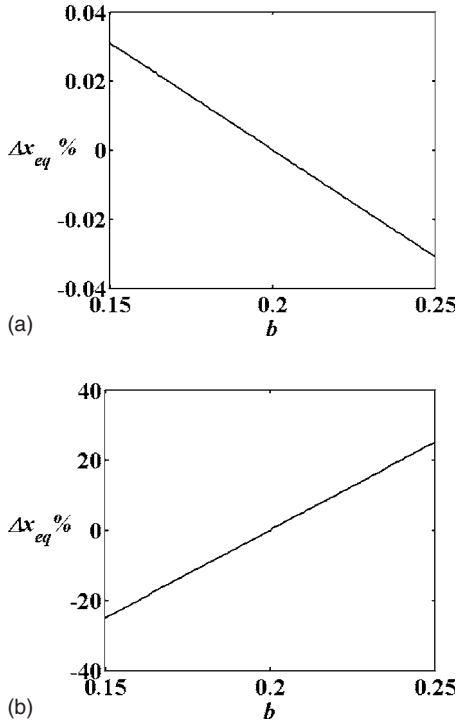

FIG. 7. Equilibrium points as a function of b. The first equilibrium point, in (a), has a maximum change of only ±0.031%, which is very small and can be practically ignored. The second equilibrium point, in (b), has a maximum change of ±25%, which is the same as the maximum change in b. Thus, the second equilibrium point is very sensitive to changes in b.

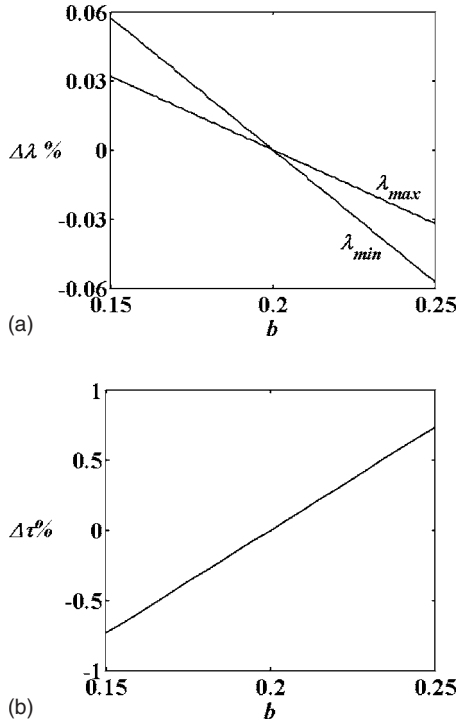

FIG. 8. The real part of the maximum/minimum Lyapunov exponents, in (a), as a function of b. The figure in (b) illustrates the effect of b on the dominant period of the Rössler system. It is demonstrated that a change in of b of ±25% resulted in a maximum change of ±0.032%, ±0.057%, and ±0.74% in λ_{max}, λ_{min}, and τ, respectively.

ments. Major contributions to overcome such difficulties are reported that use, some way or another, a controller-observer combination [19].

In the previous section, it was highlighted that the proposed controller is model-based which requires exact knowledge of both the states and the parameters of the system to be controlled. Despite the simplicity of the observer designed to reconstruct the immeasurable states of the system, it proved to be very efficient, with an adjustable convergence rate that can be easily tuned to guarantee satisfactory performance while meeting any constraints on the maximum control effort. The proposed controller assumes having a deterministic form for the model of the system to be controlled, which might not always be true. In this section, effect of parameter uncertainties is investigated by assuming that one of the system parameters, namely, b, is allowed to change within a certain range as depicted in Eq. (7). Investigating the effect of b on the controller design should be preceded by examining its effect on the equilibrium points and UPOs of the uncontrolled system. Figures 7 and 8 illustrates how the change in the uncertain parameter b is reflected on the system behavior. As shown, for a change of ±25% in b, the period of the dominant UPO changed only ±0.057%. This small change is very small to affect the closed loop of the controlled system. The control signal is now given by

$$u = -(\bar{b} + \hat{x}_1\hat{x}_3) + K[\hat{x}_1\ \hat{x}_2\ \hat{x}_3\ ]^T + k_0 y_d, \tag{18}$$

where $\bar{b}=0.2$ is the nominal value of the uncertain parameter b. When comparing Eq. (18) to Eq. (7), it is recognized that the closed loop system will suffer steady state offsets.

To quantitatively investigate the effect of the parameter uncertainty on the stability and performance of the closed loop system, the augmented controller-observer dynamics are given in Eq. (19), which should be compared to the original dynamics given in Eqs. (9) and (10).

$$\begin{bmatrix} \dot{x}_1 \\ \dot{x}_2 \\ \dot{x}_3 \\ \dot{\hat{x}}_1 \\ \dot{\hat{x}}_2 \\ \dot{\hat{x}}_3 \end{bmatrix} = \begin{bmatrix} 0 & -1 & -1 & 0 & 0 & 0 \\ 1 & a & 0 & 0 & 0 & 0 \\ 0 & 0 & -c & k_1 & k_2 & k_3 \\ 0 & \gamma_1 & 0 & 0 & -1-\gamma_1 & -1 \\ 0 & \gamma_2 & 0 & 1 & a-\gamma_2 & 0 \\ 0 & \gamma_3 & 0 & k_1 & k_2-\gamma_3 & k_3-c \end{bmatrix} \begin{bmatrix} x_1 \\ x_2 \\ x_3 \\ \hat{x}_1 \\ \hat{x}_2 \\ \hat{x}_3 \end{bmatrix} + \begin{bmatrix} 0 \\ 0 \\ k_d y_d + (b-\bar{b}) + (x_1 x_3 - \hat{x}_1\hat{x}_3) \\ 0 \\ 0 \\ k_d y_d \end{bmatrix} \tag{19}$$

Table I summarizes the statistics governing the closed loop

TABLE I. Statistics of the closed loop response and its relationship to robustness.

Case	y_d	Response Characteristics
Regulation	2	• Steady state error= ±2.31% for a change of ±25% in b. • Steady state time is the same as for $b=0.2$ (nominal value). • Control signal, u, deviates between±2.01% from its nominal value at $b=0.2$. • Uncontrolled equilibrium point shift does not affect controlled steady state. • Deviations in response are continuous and almost linear. • Estimated states: x_1 deviates±3.25% from the true value. x_2 deviates±0.06% from the true value. x_3 deviates±0.73% from the true value.
Servomechanism	2 sin(0.1t)	• Steady state error in max. amplitude= ±1.93% for a change of±25% in b. • Steady state error in min. amplitude= ±1.50% for a change of ±25% in b. • Steady state error in frequency of ±0.06% from nominal. • Steady state time is the same as for $b=0.2$ (nominal value). • Control signal, u, deviates±2.31% from its nominal value at $b=0.2$. • Uncontrolled equilibrium point shift does not controlled steady state. • Deviations in response are continuous and almost linear. • Estimated states: x_1 deviates±0.72% (max) and ±0.72% (min) from nominal. x_2 deviates±0.06% (max) and ±0.04% (min) from nominal. x_3 deviates±0.75% (max) and ±0.92% (min) from nominal.

response for the regulation and servomechanism cases, illustrating the effect of using the certainty equivalence model-based controller while the uncertain parameter is experiencing the maximum allowable change.

Thus, the closed loop system will experience a negligible shift in its equilibrium point while retaining its original stable operation. To improve the robustness of the system, the uncertain parameters should be estimated. A number of approaches can be used to accomplish such task, e.g., using adaptive techniques and synchronization methods [28,31,32].

VI. SUMMARY AND CONCLUSION

Designing model-based controllers for nonlinear chaotic systems was investigated. The unknown system states were observed and the controller parameters were adjusted using the certainty equivalence principle. The simple gradient descent method was used to force the observed states to converge to their true values using a single measurable state (the output). Careful tuning of the controller gains and observer parameters resulted in a stable and satisfactory response as illustrated by the simulations. The original system and the observer had equivalent structures, thus removing any conflict between the existence of a nonzero control signal in the feedback closed-loop system that might interact with the observer dynamics. The controller gains were systematically calculated using a pole-placement-like approach and the response followed closely the desired trajectory. When compared to both DNFF and TDAS control methods, the proposed controller proved to be superior in terms of the experimentation time needed to tune the controller parameters. In addition, the proposed controller shares the advantage of using a single time series for implementing thefeedback loop and has an order that falls between the DNFF and TDAS. Robustness analysis revealed that accommodating parameters uncertainty requires additional post-design effort to guarantee satisfactory performance of the closed loop system. Generalizing the controller application remains a challenge as nonlinear systems fall into many different classes with varying levels of dimensionality and degrees of complexity.

[1] S. Boccaletti, C. Grebogi, Y. C. Lai, H. L. Mancini, and D. Maza, Phys. Rep. **329**, 103 (2000).
[2] E. Ott, C. Grebogi, and J. Yorke, Phys. Rev. Lett. **64**, 1196 (1990).
[3] S. S. Ge and C. Wang, IEEE Trans. Circuits Syst., I: Fundam. Theory Appl. **47**, 1397 (2000).
[4] S. Boccaletti, J. Kurthsc, G. Osipovd, D. L. Valladaresb, and C. S. Zhouc, Phys. Rep. **366**, 1 (2002).
[5] M. Bernardo, Int. J. Bifurcation Chaos Appl. Sci. Eng. **6**, 557 (1996).
[6] S. S. Ge, C. Wang, and T. H. Lee, Int. J. Bifurcation Chaos Appl. Sci. Eng. **10**, 1145 (2000).

[7] A. M. Harb, A. A. Zaher, A. A. Al-Qaisia, and M. A. Zohdy, Chaos, Solitons Fractals **34**, 639 (2007).
[8] Ashraf A. Zaher, Commun. Nonlinear Sci. Numer. Simul. (to be published).
[9] Ashraf A. Zaher, J. Math. Cont. Sci. App. (to be published).
[10] Alexander Ahlborn and Ulrich Parlitz, Phys. Rev. Lett. **96**, 034102 (2006).
[11] K. Pyragas, Phys. Lett. A **170**, 421 (1992).
[12] Alexander Ahlborn and Ulrich Parlitz, Opt. Lett. **31**, 465 (2006).
[13] M. Basso, R. Genesio, and A. Tesi, IEEE Trans. Circuits Syst., I: Fundam. Theory Appl. **44**, 1023 (1997).
[14] Jonathan N. Blakely, Lucas Illing, and Daniel J. Gauthier, Phys. Rev. Lett. **92**, 193901 (2004).
[15] P. Hövel and E. Schöll, Phys. Rev. E **72**, 046203 (2005).
[16] A. G. Balanov, N. B. Janson, and E. Schöll, Phys. Rev. E **71**, 016222 (2005).
[17] K. Pyragas, Phys. Rev. Lett. **86**, 2265 (2001).
[18] H. Trinh, Int. J. Control **72**, 1642 (1999).
[19] Z. Wang, D. Goodall, and K. Burnham, Int. J. Control **75**, 803 (2002).
[20] Kohei Yamasue and Takashi Hikihara, Phys. Rev. E **69**, 056209 (2004).
[21] Alexander Ahlborn and Ulrich Parlitz, Phys. Rev. Lett. **93**, 264101 (2004).
[22] Wolfram Just, Thomas Bernard, Matthias Ostheimer, Ekkehard Reibold, and Hartmut Benner, Phys. Rev. Lett. **78**, 203 (1997).
[23] H. Khalil, *Nonlinear Systems*, 3rd ed. (Prentice Hall, New York, 2002).
[24] T. Pyragiene and K. Pyragas, Phys. Rev. E **72**, 026203 (2005).
[25] K. Pyragas, V. Pyragas, and H. Benner, Phys. Rev. E **70**, 056222 (2004).
[26] Wolfram Just, Ekkehard Reibold, Krzysztof Kacperski, Piotr Fronczak, Janusz A. Hołyst, and Hartmut Benner, Phys. Rev. E **61**, 5045 (2000).
[27] N. H. El-Farra and P. D. Christofides, Int. J. Control **74**, 133 (2001).
[28] A. M. Harb, A. A. Zaher, A. A. Al-Qaisia, and M. A. Zohdy, J. Vib. Control **9**, 623 (2003).
[29] L. Magni, Int. J. Control **75**, 399 (2002).
[30] D. L. Yu and D. Yu, Int. J. Syst. Sci. **34**, 747 (2003).
[31] Lutz Junge and Ulrich Parlitz, Phys. Rev. E **64**, 055204 (2001).
[32] K. Pyragas, V. Pyragas, I. Z. Kiss, and J. L. Hudson, Phys. Rev. E **70**, 026215 (2004).